Curr Cardiovasc Imaging Rep (2014) 7:9308
DOI 10.1007/s12410-014-9308-7

INTRAVASCULAR IMAGING (E REGAR AND U LANDMESSER, SECTION EDITORS)

# Toward Clinical μOCT—A Review of Resolution-Enhancing Technical Advances

**Kengyeh K. Chu · Giovanni J. Ughi · Linbo Liu · Guillermo J. Tearney**

Published online: 20 November 2014


**Abstract** Intravascular optical coherence tomography (IVOCT) has made significant clinical impact, providing a method of visualizing coronary plaques, optimizing percutaneous coronary intervention, and monitoring treatment results. Achieving cellular resolution in cardiovascular optical coherence tomography (OCT) adds even greater utility; thin-cap fibroatheromas (TCFA) that include microcalcifications, cholesterol crystals, and macrophages are hypothesized to correlate with rupture potential, yet are too small to be imaged by conventional OCT. In this review, we survey new developments in the optical technology that may contribute to the advancement of IVOCT into the microscopic domain, including new light sources and optical configurations. We also describe recent progress in micro-OCT (μOCT), a high-resolution OCT implementation developed in our laboratory that utilizes many of these advances to achieve 1-μm resolution.

**Keywords** Optical coherence tomography · OCT · Micro-OCT · Intravascular imaging · Macrophages · Cholesterol crystals

This article is part of the Topical Collection on *Intravascular Imaging*

K. K. Chu · G. J. Ughi · G. J. Tearney
Wellman Center for Photomedicine, Massachusetts General Hospital and Harvard Medical School, Boston, MA, USA

L. Liu
School of Electrical and Electronic Engineering, College of Engineering, Singapore, Singapore

G. J. Tearney (✉)
Department of Pathology, Massachusetts General Hospital and Harvard Medical School, Boston, MA, USA
e-mail: gtearney@partners.org

## Introduction

Optical coherence tomography (OCT) [1] has made a significant impact on cardiovascular imaging since its first demonstration in human patients over a decade ago [2, 3]. By offering resolution on the 10 μm scale, an order of magnitude improvement over intravascular ultrasound (IVUS), intravascular OCT (IVOCT) provides microscopic representations of the coronary features most relevant to the determination of their pathology. For example, IVOCT enables a detailed assessment of the atherosclerotic plaques thought to give rise to coronary events in vivo, including thin-cap fibroatheroma (TCFA), erosions, and superficial nodular calcifications [4]. In addition, IVOCT can be used to evaluate vessel healing after stent implantation, visualizing neointimal tissue covering polymer-coated or bare metallic struts [5, 6], which has been reported to be a predictor of late coronary events such as stent thrombosis and late stent failure [7]. IVOCT has also been extensively used in multiple clinical trials to assess the efficacy of novel atherosclerosis therapies [8, 9, 10•]. Today, it is being used frequently for the optimization of percutaneous coronary intervention (PCI), including guiding cardiologists to determine optimal stent placement in complex cases (such as bifurcation interventions [11•]) and for selecting better intervention parameters prior to intervention to lessen the risk of stent restenosis and thrombosis following implantation [12].

As we move toward the next generation of interventional cardiology, we now realize that we may need to be able to visualize individual cells in order to truly study atherosclerosis, make the most accurate diagnoses, and understand the pathobiological responses to implanted devices. For example, 1 major issue over the past decade has been the rare but devastating risk of developing late stent thrombosis (LST) following drug-eluting stent implantation [10•]. Histopathologic studies of patients who died of LST showed

that the single most important factor that governed this risk was coverage of the stent struts by at least a single endothelial layer [7]. If there was an imaging device that could truly assess strut coverage at this level of detail, then it could be used to manage dual-anti-platelet therapy in patients who are at risk for bleeding complications. Since endothelial cells are at most 2 μm thick, conventional IVOCT, with its resolution of 10 μm, cannot make this assessment. We must instead have OCT with resolution in the 1–2 μm range.

Another example where higher resolution intravascular imaging could be an advantage is improved identification of vulnerable plaque that by definition will go on to cause a coronary event. Histopathology studies have taught us that the main type of vulnerable plaque is a thin-capped fibroatheroma, comprising a thin (<65 μm), collagen-rich cap that overlies a necrotic lipid core [13]. Even though this definition of vulnerable is well established, it must not be complete because evidence from multiple imaging and autopsy studies show that patients may have many such plaques that never cause a coronary event [14]. Hypotheses exist that attempt to refine which TCFA actually do go on to rupture, including the presence of cap micro-calcifications [15], cholesterol crystals [16], and activated macrophages [17], but these entities cannot be visualized by conventional OCT. So, if we are to be able to someday have the best chance to predict which coronary plaques will progress to culprit lesions, we will likely need 1–2 μm subcellular resolution to do so.

Unfortunately, the resolution of OCT lags that of conventional optical techniques because of a "catch-22" that forces a trade-off in resolution and field-of-view. In microscopy, the angle of convergence of light determines numerical aperture (NA). In conventional microscopes, a high NA is unequivocally desirable, because a high NA generates a small focal spot, well-confined both horizontally and vertically, which translates to high resolution, both laterally and axially. However, because OCT is a depth-ranging modality, the ideal focus would be narrow laterally but as long and deep as possible to capture a long field of view. NA is not relevant to OCT depth resolution, which comes from the coherence properties of the light source, not from the shape of the focus. Unfortunately, these 2 requirements are at odds with one another, because a high NA is needed for good lateral resolution, but a low NA is needed to produce a reasonably long depth of focus. Most OCT systems strike a balance more in favor of the depth of focus, which is necessary to image the diverse morphology and lumen diameters that may be encountered in the coronaries, especially in diseased arteries. Figure 1 shows the beam profiles generated by high NA and low NA optics, demonstrating the trade-off necessary to achieve reasonable field-of-view in the axial direction.

Clinical cardiovascular OCT has shifted in favor of Fourier-Domain OCT (FD-OCT), in place of the former standard Time-Domain OCT (TD-OCT) owing to its tremendous

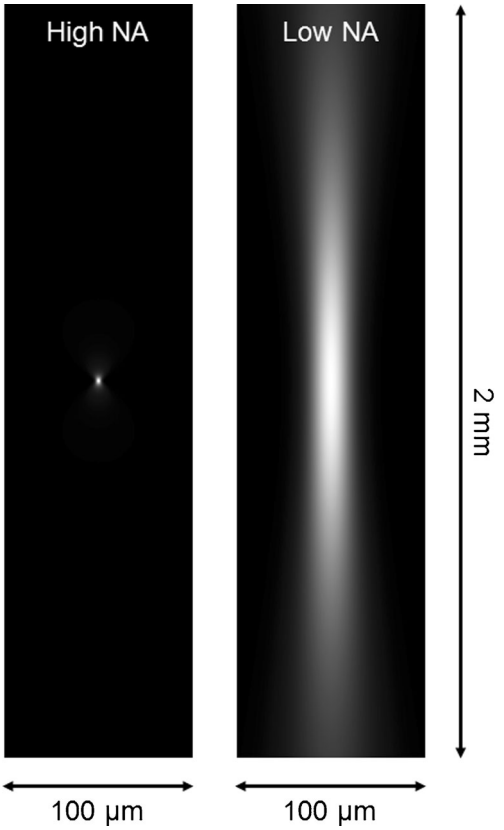


**Fig. 1** Beam profiles illustrating lateral resolution and depth-of-focus trade-off in OCT. *Left*, high NA focus generating 4 μm diameter beam but depth-of-focus is only 19 μm. *Right,* low NA focus generating 30 μm diameter beam and depth-of-focus is 0.5 mm

gain in scanning speed, a critical feature when imaging a small space under constant motion. There are 2 incarnations of FD-OCT, both of which operate by measuring the spectrum of broadband OCT interference. Swept-source OCT (SS-OCT), also known as Optical Frequency Domain Imaging (OFDI), uses a narrow band laser that changes the wavelength of its emission over time, and, thus, allows a spectrum to be measured as a function of time [18, 19]. Spectral-domain OCT (SD-OCT) employs a light source that emits all wavelengths at a time, and a spectrometer is used to measure the spectrum [20]. Of these 2 forms, SS-OCT/OFDI is the predominant version used in cardiovascular settings, since the type of detectors used in SS-OCT/OFDI tend to be faster and more resistant to motion artifacts. Because all forms of OCT derive axial resolution from the broadness of the illumination source, the development of frequency sweeping lasers that cover a wider range of wavelengths and new broadband coherent light sources are beneficial to the resolution of SS-OCT/OFDI and SD-OCT, respectively.

Resolution also scales with optical wavelength. Based primarily on the availability of appropriate light sources and detectors, OCT is dominated by 2 wavelength ranges: 800 nm and 1300 nm. Clinical cardiovascular OCT is performed almost exclusively in the 1300 nm range, which

confers many advantages including the ability to penetrate deeply into tissue, but sacrifices resolution because of its comparatively long wavelength.

This review will highlight recent technical efforts with the potential to improve cardiovascular OCT resolution in 3 categories: (1) OCT-capable light sources at shorter wavelengths, (2) new super-broadband OCT light sources, and (3) solving the resolution/field-of-view dilemma. Finally, we will discuss technique progress on micro-OCT (μOCT), a technical recently developed in the authors' laboratory which utilizes all 3 categories to achieve 2 μm lateral and 1 μm axial resolution.

## OCT Light Sources Emitting Wavelengths Shorter than 1300 nm

Though there are many compelling reasons to choose the 1300 nm window for cardiovascular OCT, including better penetration into the artery wall, the argument for the shorter and higher resolution 800 nm band has been more or less academic owing to the lack of swept source laser options in the 800 nm range. The search has been limited to swept sources because OFDI/SS-OCT has been traditionally preferred to SD-OCT for the high motion imaging environment of the coronary arteries. This is due to superior resistance to a type of motion artifact known as fringe washout, resulting from relatively slow SD-OCT spectrometer cameras.

Several research groups have reported 800 nm swept laser sources in the past several years. Lim et al utilized 800 nm OFDI in 2006 [21] but a relatively small bandwidth limited the resolution to 10 μm. Srinivasan et al later demonstrated a 850 nm swept source with 7 μm resolution for ophthalmic OCT [22]. However, there has been no widespread adoption of 800 nm swept sources for cardiovascular OCT, as the reduced bandwidths of these sources result in only marginal improvements in resolution, which is not compelling enough to offset the disadvantages of 800 nm.

The 1000 nm (1 μm) wavelength range has also been developed for ophthalmic OCT. This spectral region is largely unexplored for cardiovascular imaging, though it likely represents a compromise between the higher resolution at 800 nm and the improved penetration of 1300 nm.

E. Lee et al reported a 1060 nm OFDI system for choroid imaging [23]. A 1050 nm swept laser has also been produced by Axsun Technologies (Billerica, MA) was used by Potsaid et al [24] to achieve 5.3 μm axial resolution. S. Lee et al have also developed a 1020 nm scanning system with 2.9 μm resolution, with an example of in vivo ultrahigh-resolution retinal imaging [25].

It is also possible to convert pulsed light, which inherently contains many spectral components, into a swept-source-like chirped pulse by sending the pulse through a length of optical fiber that exhibits dispersion [26]. The fiber will slow the wavelengths in the pulse by differing amounts, thus approximating swept-source laser output. However, such a configuration has drawbacks, such as a requirement for very long dispersive fibers (several kilometers) and a very low spectral noise pulsed laser [27], both of which limit clinical applicability.

Though conventional wisdom favors SS-OCT/OFDI, much faster array detectors are available today than at the inception of cardiovascular OCT, reducing the impact of fringe washout and opening the door for SD-OCT in cardiovascular applications and enabling a much broader class of lasers and other broadband sources to be considered, including those near 800 nm. Many of these will be discussed in the following section.

## Ultra-Broadband OCT Sources

There are several classes of broadband light sources undergoing continuous development with important impacts on OCT. We will review 3: pulsed lasers, supercontinuum lasers, and swept sources.

Lasers generating extremely short pulses on a femtosecond time scale are also inherently broadband. Titanium sapphire lasers, whose short and intense pulses are convenient for nonlinear microscopies, have also been used for high-resolution OCT [28, 29]. Ti:sapphire lasers optimized specifically for spectral breadth have been produced with 400 nm bandwidths [30], but high cost and limited portability of these sources have likely prevented clinical application.

An entirely new branch of sources, supercontinuum lasers, produce spectra that are astonishingly broad. These lasers are commonly called "white-light lasers" because of their multispectral nature, but their output often stretches far into the infrared. Supercontinuum lasers utilize a specialized fiber that causes pulsed light to broaden spectrally as it propagates. The earliest examples were too noisy for OCT imaging, but several groups developed homemade supercontinuum lasers for OCT [31–33] about a decade ago. New commercial sources from manufacturers such as Fianium (Southampton, England, UK) [34, 35] and NKT Photonics (Birkerod, Denmark) [36, 37] have proven to be turnkey solutions with suitably low laser noise for high-sensitivity OCT applications.

Development is also ongoing to extend the bandwidth of tunable wavelength-swept lasers of the type currently used in OFDI/SS-OCT systems. A tunable laser's bandwidth is usually limited by the semiconductor amplifier, which essentially stores photons in the form of electronic energy, ready to emit as laser radiation. Typical amplifiers in current OFDI/SS-OCT systems operate within about a 100 nm breadth centered near 1300 nm. To extend this bandwidth, Jeon et al [38] introduced a system using 2 semiconductor gain components to achieve 160 nm spectral width, giving an OFDI resolution of 4.7 μm in tissue. Jang et al more recently extended the dual amplifier approach to produce a swept laser source with 210 nm tuning

range [39]. The wavelengths and bandwidths of these recently developed swept sources are listed in Table 1.

## Resolving the Depth of Field Dilemma

With the potential to improve axial resolution an order of magnitude to submicron levels by the use of high bandwidth sources, a parallel gain in the lateral direction is needed to achieve high resolution OCT. The limiting factor in cardiovascular OCT lateral resolution is typically the design choice of low NA optics to generate a long field of view to cope with the diverse vessel morphologies that may be encountered. Nonstandard beam geometries can alleviate the tradeoff between depth of field and lateral resolution, a few of which will be explored below.

One such method is to use a Bessel beam shape. In contrast to a standard beam in which light covering the entire objective lens is focused to a single position, a Bessel beam is formed by a cone-shaped lens (axicon) resulting in foci at a range of axial positions. OCT has been implemented with Bessel beams [40, 41] that demonstrated improved depth of focus at relatively high NAs, and endoscopic probes have also been successfully fabricated with Bessel optics [42, 43]. Figure 2, reprinted from [41], illustrates the degree to which Bessel optics can preserve high resolution over an extended depth of field. However, Bessel beam OCT images are hindered by the presence of side-lobe artifacts, spurious ring-like features that surround point objects. The side-lobes are deleterious to image interpretation and also reduce the power contained in the main focus, limiting sensitivity. A phase pattern that delays light in ring patterns has also been shown to enhance depth of focus without sacrificing as much sensitivity [44].

Another recently reported approach known as Interferometric Synthetic Aperture Microscopy (ISAM) utilizes image information from multiple columns to computationally "refocus" the OCT system to arbitrary positions [45]. However, because ISAM requires imaging data from multiple scan positions, a high degree of stability is required. ISAM is relatively slow because of its computational intensity, though algorithm optimizations have greatly improved its speed [46]. ISAM has now been demonstrated in vivo for dermatology [47], and following the current trajectory of computational power, may soon be robust enough for the even higher motion environment of the coronary arteries, though miniaturization of the ISAM components will remain a significant challenge.

A method of using multiple apertures that can be recombined in-phase to virtually refocus has also been recently demonstrated [48]. This technique requires minimal additionally processing and does not require integrated data from multiple scan positions. The multiple apertures can be multiplexed into a single device, and thus, is amenable to development as a catheter probe.

## Micro-OCT: 1-μm Axial, 2-μm Lateral Resolution OCT

Our laboratory has developed an implementation of OCT that integrates elements of all 3 of the above-described resolution enhancement strategies, using light centered at 800 nm with extreme breadth from a supercontinuum laser combined with an aperture shape that enhances the axial depth of scan. We have termed this technology Micro-OCT (μOCT).

The means by which the enhanced spectrum from our supercontinuum source improves resolution has already been described above. Various iterations have used lasers from both NKT Photonics A/S and Fianium Ltd. μOCT is configured as a SD-OCT, using a spectrometer to measure the OCT interferogram. The silicon-based spectrometer detector limits μOCT detection to 1000 nm and below, though the output of the supercontinuum sources extends to 1800 nm and beyond.

The NA of μOCT is high for OCT (NA =0.12). The depth-of-focus enhancing component is achieved by introducing a circular obscuration that blocks the center of the OCT illumination beam such that the remaining light is a hollow annular shape. This geometry can be considered a blend between normal optics and the depth-of-focus enhancing Bessel

**Table 1** List of recently developed swept laser sources with resolution <10 μm

| Center wavelength (nm) | Bandwidth (nm) | Axial resolution/coherence length (μm in water/tissue) | Date | Authors/vendor |
|---|---|---|---|---|
| 850 | 35 | 6.8 | 2007 | Srinivasan et al [22] |
| 1060 | 62 | 6.0 | 2006 | E. Lee et al [23] |
| 1060 | ~100 | 5.3 | 2010 | Potsaid et al [24]/Axsun Technologies |
| 1300 | 136.5 | 4.7 | 2008 | Jeon et al [38] |
| 1020 | 121.5 | 2.9 | 2011 | S. Lee et al [25] |
| 1270 | 210 | 4.5 (reported)<br>2.8 (theoretical) | 2013 | Jang et al [39] |

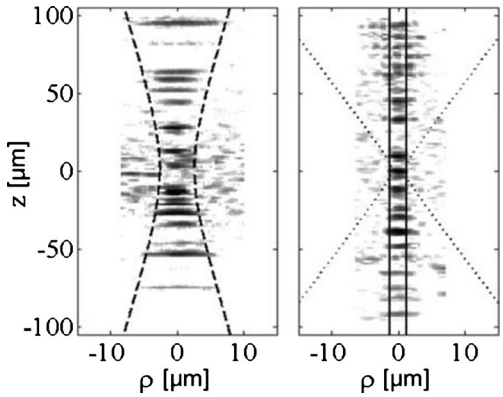


**Fig. 2** Reprinted from Leitgeb et al [41]. OCT images of 1-μm beads as a function of axial position, comparing conventional optics in which beads away from focus are blurred (*left*) and a Bessel-like beam geometry, where high resolution is preserved ±100 μm away from focus (*right*)

pattern, and its optical properties are likewise a mix: depth-of-focus is increased substantially though not to the same degree as a pure Bessel, and sidelobe artifacts and sensitivity loss are also tempered. In μOCT the demonstrated lateral resolution is 2 μm, axial resolution is 1 μm, and depth-of-focus is approximately 300 μm [49••].

We have previously demonstrated ex vivo and in vitro imaging using μOCT [49••, 50]. Examples of μOCT imaging appear in Fig. 3. Because of its subcellular resolution, μOCT was able to observe endothelial pavementing, leukocytes, thrombi (including platelets and fibrin) and foam cells in human cadaver coronaries. Plaques were imaged with sufficient detail to visualize microcalcifications and individual cholesterol crystals (Fig. 4). In particular, macrophages and cholesterol crystals are below the resolution threshold of current cardiovascular OCT, but theorized to play active roles in atherogenesis [51].

The first generation of μOCT endoscopic probes is now under development. The miniaturization of μOCT is confronted by 2 key technical challenges: (1) the annular beam shape must be made by a novel element within the probe, and (2) dispersion must be kept very low to preserve high axial resolution.

The annular beam shape, which is made by a 3 mm component in the benchtop μOCT system, must be generated by a much more compact arrangement for a catheter device. In the prototype probe, a beam-splitter prism is coated with gold to reflect light at a right angle toward the sample, but a circular defect in the reflective coating is carefully applied at the center. An annular beam is generated by light reflecting off of the coated portion surrounding the defect.

The other difficulty is dispersion management. A mismatch between the sample and reference arms in the material type or in the amount of the same material can lead to dispersion, a resolution-compromising result of different wavelengths of light having traveled different distances. Typical 1300 nm OCT tolerates sample/reference fiber length differences relatively well because the glass is minimally dispersive at 1300 nm; so long as

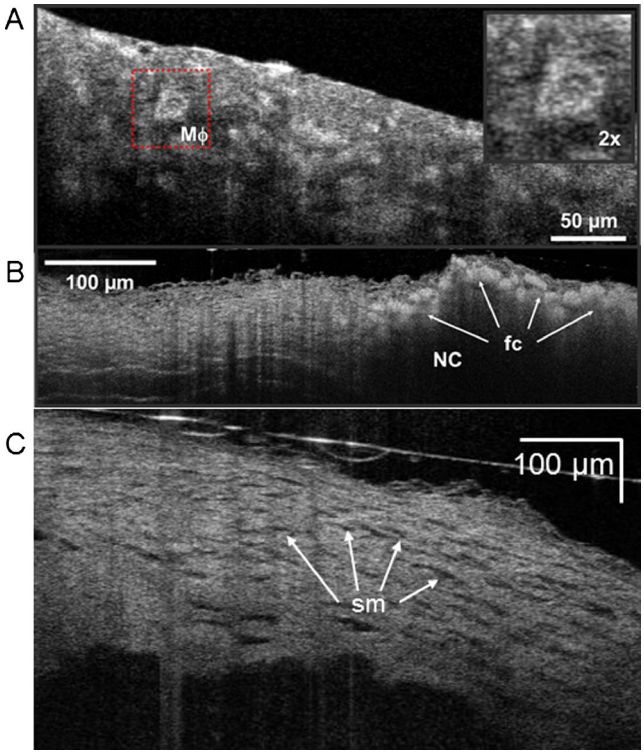


**Fig. 3** 1-μm axial/2-μm lateral resolution μOCT images of human coronary tissue ex vivo. **A**, A macrophage (MΦ) is visible within a plaque, including a dark center region, which may be the nucleus. **B**, reprinted from [49••]. Foam cells (fc) infiltrate a necrotic core (nc) fibroatheroma. **C**, spindle-shaped smooth muscle cells (sm).

the reference fiber is within a few millimeters in length as the catheter fiber, OFDI imaging is not significantly degraded. Unfortunately, μOCT is far more sensitive to dispersion. Glass

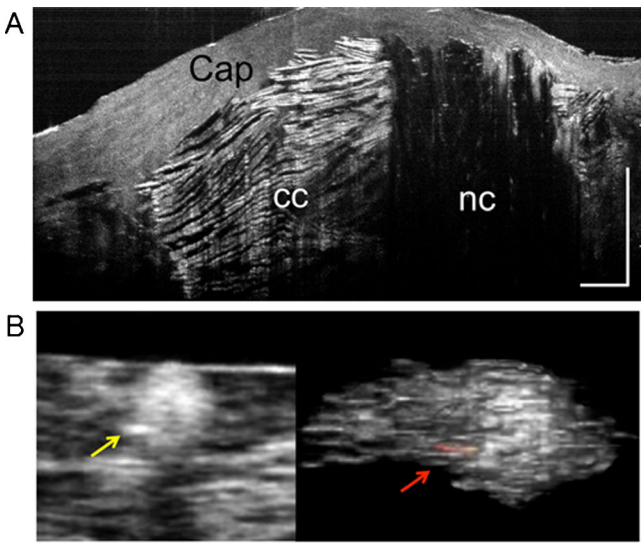


**Fig. 4** μOCT images of cholesterol crystals. **A**, reprinted from [49••]. Large necrotic core (nc) fibroatheroma, showing cholesterol crystals (cc), scale bar =100 μm. **B**, Reprinted from [50]. *Left*, macrophage containing a highly scattering inclusion that may be a cholesterol crystal. *Right*, 3D rendering of macrophage highlighting a scattering inclusion in red

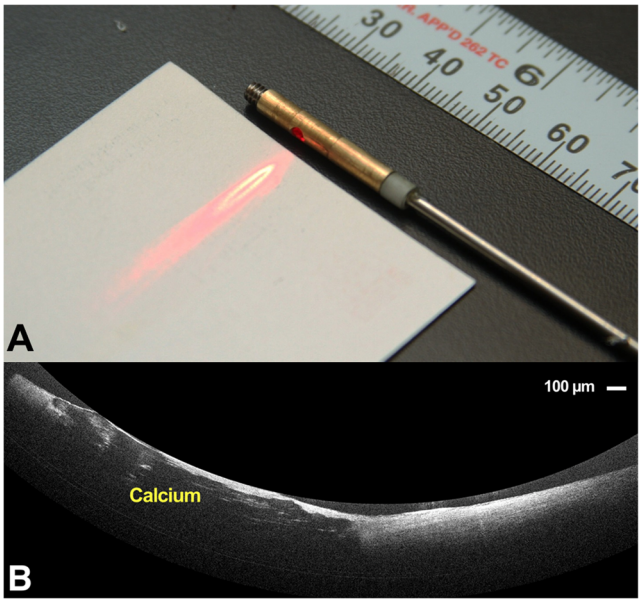


**Fig. 5** Early μOCT probe development. **A**, 2 mm prototype projecting annular μOCT beam geometry. **B**, partial μOCT scan of a human carotid plaque, obtained ex vivo, showing arterial tissue measurements with 1 μm resolution

dispersion is much stronger in the 800 nm region and is exacerbated by the very broad μOCT spectrum. Furthermore, because the resolution is high, even a small amount of blurring caused by dispersion will erode μOCT image quality. To ensure optimal balance between sample and reference arms, the reference is built within the μOCT probe itself to minimize the difference in the path traveled by the 2 beams, which is known as a common-path design [52]. Fortunately, the circularly masked prism used to generate the annular μOCT beam is highly amenable to a common-path configuration; the light that strikes the uncoated center portion of the beam-splitter prism is simply transmitted toward a reference reflector.

This first generation μOCT probe has been used in preliminary validation experiments in swine airways [53]. Figure 5 shows an early prototype and image from an ex vivo artery. Further development to miniaturize μOCT technology to coronary catheter sizes is ongoing.

## Conclusions

The value of enhanced imaging resolution for intracoronary OCT is clear; some of the most pressing questions in atherosclerosis research can be interrogated with an in vivo imaging technology with subcellular resolution. This review has briefly surveyed some of the latest technical developments that have improved resolving power in other clinical fields including dermatology and ophthalmology that have the potential to be adapted to clinically feasible high-resolution intravascular OCT. Shorter wavelength semiconductor-based swept lasers are amenable to clinical use in terms of portability and affordability, and while their use in coronary imaging is largely unexplored, the higher resolution compared to 1300 nm and longer penetration compared to 800 nm seems to strike a reasonable balance of imaging requirements. New ultrabroadband laser sources offer improved axial resolution. In particular, supercontinuum sources which formerly required exotic laser setups that constrained them to research settings are now available as portable turnkey solutions. Meanwhile, new strategies for overcoming the depth-of-focus tradeoff also promise better lateral resolution while preserving a reasonable field of view. We have also summarized our lab's μOCT research, in which we have utilized new techniques on each of these fronts to develop an endoscopic μOCT probe.

Future iterations of this technology will result in an intracoronary catheter capable of imaging plaque microstructure at a resolution of 1 μm. This advance will fundamentally change how we are able to see coronary artery disease, a change that will bring us to the cells that initiate and propagate this problem. With this level of detail, we will be able to determine with confidence what plaques are likely to rupture, what therapeutic strategies are most effective at mitigating risk, and how individual patients respond to their treatment.

### Compliance with Ethics Guidelines

**Conflict of Interest** Kengyeh K. Chu has a patent WO Patent 2,013,029,047 pending, and a patent PCT/US2013/073891 pending. Giovanni Ughi declares that he has no conflict of interest. Linbo Liu has a patent US Patent App. 13/042,230 pending, a patent EP Patent 2,542,153 pending, and a patent WO Patent 2,013,029,047 pending. Guillermo J. Tearney (Massachusetts General Hospital) has patent licensing arrangements with Terumo Corporation and NinePoint Medical. Tearney has the right to receive licensing income from these licensing agreements. Tearney receives consulting income from Samsung and NinePoint Medical. Tearney receives sponsored research from Canon, NinePoint Medical, and Samsung. Tearney receives NIH research grants (R01HL093717 and R01HL076398).

**Human and Animal Rights and Informed Consent** Imaging studies of human arterial specimens was performed with approval of the Massachusetts General Hospital Institutional Review Board (IRB # #2004P000578).

## References

Papers of particular interest, published recently, have been highlighted as:
- • Of importance
- •• Of major importance

1. Huang D, Swanson EA, Lin CP, Schuman JS, Stinson WG, Chang W, et al. Optical coherence tomography. Science. 1991;254:1178–81.

2. Jang IK, Bouma BE, Kang DH, Park SJ, Park SW, Seung KB, et al. Visualization of coronary atherosclerotic plaques in patients using optical coherence tomography: comparison with intravascular ultrasound. J Am Coll Cardiol. 2002;39:604–9.
3. Yabushita H, Bouma BE, Houser SL, Aretz HT, Jang IK, Schlendorf KH, et al. Characterization of human atherosclerosis by optical coherence tomography. Circulation. 2002;106:1640–5.
4. Jia H, Abtahian F, Aguirre AD, Lee S, Chia S, Lowe H, et al. In vivo diagnosis of plaque erosion and calcified nodule in patients with acute coronary syndrome by intravascular optical coherence tomography. J Am Coll Cardiol. 2013;6:1748–58. doi:10.1016/j.jacc.2013.05.071.
5. Matsumoto D, Shite J, Shinke T, Otake H, Tanino Y, Ogasawara D, et al. Neointimal coverage of sirolimus-eluting stents at 6-month follow-up: evaluated by optical coherence tomography. Eur Heart J. 2007;28:961–7.
6. Takano M, Inami S, Jang I-K, Yamamoto M, Murakami D, Seimiya K, et al. Evaluation by optical coherence tomography of neointimal coverage of sirolimus-eluting stent three months after implantation. Am J Cardiol. 2007;99:1033–8.
7. Finn AV, Joner M, Nakazawa G, Kolodgie F, Newell J, John MC, et al. Pathological correlates of late drug-eluting stent thrombosis strut coverage as a marker of endothelialization. Circulation. 2007;115:2435–41.
8. Chia S, Raffel OC, Takano M, Tearney GJ, Bouma BE, Jang IK. Association of statin therapy with reduced coronary plaque rupture: an optical coherence tomography study. Coron Artery Dis. 2008;19:237–42. doi:10.1097/MCA.0b013e32830042a800019501-200806000-00004.
9. Takarada S, Imanishi T, Kubo T, Tanimoto T, Kitabata H, Nakamura N, et al. Effect of statin therapy on coronary fibrous-cap thickness in patients with acute coronary syndrome: assessment by optical coherence tomography study. Atherosclerosis. 2009;202:491–7.
10.• Guagliumi G, Costa MA, Sirbu V, Musumeci G, Bezerra HG, Suzuki N, et al. Strut coverage and late malapposition with paclitaxel-eluting stents compared with bare metal stents in acute myocardial infarction: optical coherence tomography substudy of the Harmonizing Outcomes with Revascularization and Stents in Acute Myocardial Infarction (HORIZONS-AMI) Trial. Circulation. 2011;123:274–81. doi:10.1161/CIRCULATIONAHA.110.963181. *This work establishes an important connection between drug-eluting stents and uncovered or malapposed stent struts using an IVOCT trial.*
11.• Farooq V, Gogas BD, Okamura T, Heo JH, Magro M, Gomez-Lara J, et al. Three-dimensional optical frequency domain imaging in conventional percutaneous coronary intervention: the potential for clinical application. Eur Heart J. 2013;34:875–85. doi:10.1093/eurheartj/ehr409. *This is the first publication to directly evaluate the clinical application and relevance of 3D IVOCT.*
12. Guagliumi G, Sirbu V, Musumeci G, Gerber R, Biondi-Zoccai G, Ikejima H, et al. Examination of the in vivo mechanisms of late drug-eluting stent thrombosis: findings from optical coherence tomography and intravascular ultrasound imaging. JACC: Cardiovasc Intervent. 2012;5:12–20.
13. Virmani R, Burke AP, Kolodgie FD, Farb A. Vulnerable plaque: the pathology of unstable coronary lesions. J Intervention Cardiol. 2002;15:439–46.
14. Virmani R, Kolodgie FD, Burke AP, Farb A, Schwartz SM. Lessons from sudden coronary death: a comprehensive morphological classification scheme for atherosclerotic lesions. Arterioscler Thromb Vasc Biol. 2000;20:1262–75.
15. Kelly-Arnold A, Maldonado N, Laudier D, Aikawa E, Cardoso L, Weinbaum S. Revised microcalcification hypothesis for fibrous cap rupture in human coronary arteries. Proc Natl Acad Sci U S A. 2013;110:10741–6. doi:10.1073/pnas.1308814110.
16. Tian J, Ren X, Vergallo R, Xing L, Yu H, Jia H, et al. Distinct morphological features of ruptured culprit plaque for acute coronary events compared to those with silent rupture and thin-cap fibroatheroma: a combined optical coherence tomography and intravascular ultrasound study. J Am Coll Cardiol. 2014;63:2209–16. doi:10.1016/j.jacc.2014.01.061.
17. Kolodgie FD, Virmani R, Burke AP, Farb A, Weber DK, Kutys R, et al. Pathologic assessment of the vulnerable human coronary plaque. Heart. 2004;90:1385–91. doi:10.1136/hrt.2004.041798.
18. Yun S, Tearney G, de Boer J, Iftimia N, Bouma B. High-speed optical frequency-domain imaging. Opt Express. 2003;11:2953–63.
19. Tearney GJ, Waxman S, Shishkov M, Vakoc BJ, Suter MJ, Freilich MI, et al. Three-dimensional coronary artery microscopy by intracoronary optical frequency domain imaging. JACC Cardiovasc Imaging. 2008;1:752–61. doi:10.1016/j.jcmg.2008.06.007.
20. Häusler G, Lindner MW. "Coherence radar" and "spectral radar"—new tools for dermatological diagnosis. J Biomed Opt. 1998;3:21–31.
21. Lim H, De Boer J, Park B, Lee E, Yelin R, Yun S. Optical frequency domain imaging with a rapidly swept laser in the 815–870 nm range. Opt Express. 2006;14:5937–44.
22. Srinivasan VJ, Huber R, Gorczynska I, Fujimoto JG, Jiang JY, Reisen P, et al. High-speed, high-resolution optical coherence tomography retinal imaging with a frequency-swept laser at 850 nm. Opt Lett. 2007;32:361–3.
23. Lee EC, de Boer JF, Mujat M, Lim H, Yun SH. In vivo optical frequency domain imaging of human retina and choroid. Opt Express. 2006;14:4403–11.
24. Potsaid B, Baumann B, Huang D, Barry S, Cable AE, Schuman JS, et al. Ultrahigh speed 1050 nm swept source/Fourier domain OCT retinal and anterior segment imaging at 100,000 to 400,000 axial scans per second. Opt Express. 2010;18:20029–48. doi:10.1364/OE.18.020029.
25. Lee SW, Song HW, Jung MY, Kim SH. Wide tuning range wavelength-swept laser with a single SOA at 1020 nm for ultrahigh resolution Fourier-domain optical coherence tomography. Opt Express. 2011;19:21227–37. doi:10.1364/OE.19.021227.
26. Walewski J, Sanders S. High-resolution wavelength-agile laser source based on pulsed super-continua. Appl Phys B. 2004;79:415–8.
27. Yun SH, Bouma BE. Wavelength swept lasers. In: Drexler W, Fujimoto JG, editors. Optical coherence tomography: technology and applications. Berlin: Springer-Verlag; 2008. p. 359–77.
28. Bouma B, Tearney GJ, Boppart SA, Hee MR, Brezinski ME, Fujimoto JG. High-resolution optical coherence tomographic imaging using a mode-locked Ti:Al(2)O(3) laser source. Opt Lett. 1995;20:1486–8.
29. Wojtkowski M, Srinivasan V, Ko T, Fujimoto J, Kowalczyk A, Duker J. Ultrahigh-resolution, high-speed, Fourier domain optical coherence tomography and methods for dispersion compensation. Opt Express. 2004;12:2404–22.
30. Morgner U, Kärtner F, Cho S-H, Chen Y, Haus HA, Fujimoto JG, et al. Sub-two-cycle pulses from a Kerr-lens mode-locked Ti:sapphire laser. Opt Lett. 1999;24:411–3.
31. Wang Y, Zhao Y, Nelson J, Chen Z, Windeler RS. Ultrahigh-resolution optical coherence tomography by broadband continuum generation from a photonic crystal fiber. Opt Lett. 2003;28:182–4.
32. Marks DL, Oldenburg AL, Reynolds JJ, Boppart SA. Study of an ultrahigh-numerical-aperture fiber continuum generation source for optical coherence tomography. Opt Lett. 2002;27:2010–2.
33. Povazay B, Bizheva K, Unterhuber A, Hermann B, Sattmann H, Fercher AF, et al. Submicrometer axial resolution optical coherence tomography. Opt Lett. 2002;27:1800–2.

34. Kray S, Grychtol P, Hermes B, Bornemann J, Kurz H. Simultaneous dual-band ultra-high resolution optical coherence tomography. Opt Express. 2007;15:10832–41.
35. WhiteLase SC480: Ultra High-Power Supercontinuum Fiber Laser. Available at: http://www.fianium.com/pdf/WhiteLase_SC480_BrightLase_v1.pdf. Accessed Aug 8, 2014.
36. Cimalla P, Walther J, Mehner M, Cuevas M, Koch E. Simultaneous dual-band optical coherence tomography in the spectral domain for high resolution in vivo imaging. Opt Express. 2009;17:19486–500.
37. SuperK EXTREME: High Power Supercontinuum Fiber Laser Series. Available at: http://www.nktphotonics.com/files/files/SuperK_EXTREME.pdf. Accessed Aug 8, 2014.
38. Jeon MY, Zhang J, Wang Q, Chen Z. High-speed and wide bandwidth Fourier domain mode-locked wavelength swept laser with multiple SOAs. Opt Express. 2008;16:2547–54.
39. Jang W, Lim J, Kim H, Ha J. Broadband wavelength swept source combining a quantum dot and a quantum well SOA in the wavelength range of 1153–1366 nm. Electron Lett. 2013;49:1205–6.
40. Ding Z, Ren H, Zhao Y, Nelson JS, Chen Z. High-resolution optical coherence tomography over a large depth range with an axicon lens. Opt Lett. 2002;27:243–5.
41. Leitgeb R, Villiger M, Bachmann A, Steinmann L, Lasser T. Extended focus depth for Fourier domain optical coherence microscopy. Opt Lett. 2006;31:2450–2.
42. Lee K-S, Rolland JP. Bessel beam spectral-domain high-resolution optical coherence tomography with micro-optic axicon providing extended focusing range. Opt Lett. 2008;33:1696–8.
43. Lorenser D, Yang X, Sampson DD. Ultrathin fiber probes with extended depth of focus for optical coherence tomography. Opt Lett. 2012;37:1616–8.
44. Liu L, Liu C, Howe WC, Sheppard CJ, Chen N. Binary-phase spatial filter for real-time swept-source optical coherence microscopy. Opt Lett. 2007;32:2375–7.
45. Ralston TS, Marks DL, Carney PS, Boppart SA. Interferometric synthetic aperture microscopy. Nat Phys. 2007;3:129–34.
46. Ralston TS, Marks DL, Carney PS, Boppart SA. Real-time interferometric synthetic aperture microscopy. Opt Express. 2008;16:2555–69.
47. Ahmad A, Shemonski ND, Adie SG, Kim HS, Hwu WM, Carney PS, et al. Real-time in vivo computed optical interferometric tomography. Nat Photon. 2013;7:444–8. doi:10.1038/nphoton.2013.71.
48. Mo J, de Groot M, de Boer JF. Focus-extension by depth-encoded synthetic aperture in Optical Coherence Tomography. Opt Express. 2013;21:10048–61. doi:10.1364/OE.21.010048.
49.•• Liu L, Gardecki JA, Nadkarni SK, Toussaint JD, Yagi Y, Bouma BE, et al. Imaging the subcellular structure of human coronary atherosclerosis using micro-optical coherence tomography. Nat Med. 2011;17:1010–4. doi:10.1038/nm.2409nm.2409. *This work represents the highest resolution OCT imaging of coronary arteries known to date*.
50. Kashiwagi M, Liu L, Chu KK, Sun CH, Tanaka A, Gardecki JA, et al. Feasibility of the assessment of cholesterol crystals in human macrophages using micro optical coherence tomography. PLoS One. 2014;9:e102669. doi:10.1371/journal.pone.0102669.
51. Duewell P, Kono H, Rayner KJ, Sirois CM, Vladimer G, Bauernfeind FG, et al. NLRP3 inflammasomes are required for atherogenesis and activated by cholesterol crystals. Nature. 2010;464:1357–61. doi:10.1038/nature08938.
52. Vakhtin AB, Kane DJ, Wood WR, Peterson KA. Common-path interferometer for frequency-domain optical coherence tomography. Appl Opt. 2003;42:6953–8.
53. Chu KK, Carruth RW, Singh K, Ma H, Winkelmann J, Rowe SM, et al. Linear scanning micro-optical coherence tomography probe for imaging of mucociliary transport in airways. San Francisco: SPIE Photonics West; 2014.